Computation of aerodynamic damping for wind turbine applications

Bertagnolio, Franck; Gaunaa, Mac; Hansen, M.; Sørensen, Niels N.; Rasmussen, Flemming

Published in:
CD-Rom proceedings

Publication date:
2002

Document Version
Publisher's PDF, also known as Version of record

4th GRACM Congress on Computational Mechanics
GRACM 2002
Patras, 27-29 June, 2002

COMPUTATION OF AERODYNAMIC DAMPING FOR WIND TURBINE APPLICATIONS

Franck Bertagnolio, Mac Gaunaa, Morten Hansen
Niels Sørensen, and Flemming Rasmussen

Wind Energy Department
Risø National Laboratory
P.O. Box 49, DK-4000 Roskilde, Denmark
e-mail: franck.bertagnolio@risoe.dk, web page: http://www.risoe.dk/vea

Keywords: Computational Fluid Dynamics, Structural Dynamics, Fluid-Structure Interaction, Aeroelasticity, Damping, Wind Turbine, Rotor Simulation.

Abstract: *This work focuses on the numerical evaluation of aerodynamic damping for a wind turbine rotor. A finite beam element code is used to describe the structure. Two types of aerodynamic models are compared. Firstly, two engineering dynamic stall models are already implemented in the structural code for modelling the aerodynamic forces. Secondly, a Navier-Stokes flow solver has been coupled to the structural model. Test cases involving a two-bladed wind turbine rotor are performed. The aerodynamic damping is computed for the two first eigenmodes of the structure. A comparison study of the results highlights the discrepancies between the different aerodynamic models.*

1 INTRODUCTION

Wind turbines operating in the stalled condition have in some cases during recent years experienced problems with severe blade vibrations in particular in the edgewise mode shape. The problem is designated stall induced vibrations and is associated with low or even negative aerodynamic damping. Aeroelastic simulations have not been able to predict the phenomenon with sufficient reliability or the interpretation of the results has been lacking. This is due to high complexity of the problem and the dependency on a large number of parameters. Much reseach effort has been dedicated to this subject. This has revealed that the main parameters determining the aerodynamic damping, are the effective vibration direction of the blades (i.e. the mode shapes) and the static and dynamic stall characteristics, in particular the effective slope of the dynamic stall loops.

This paper is dealing with the computation of aerodynamic damping by means of two different approaches. The semi-empirical dynamic stall models are commonly used in the aeroelastic predictions in order to predict the aerodynamic loads. However, they are relatively simplified models of the actual fluid flow dynamics around the airfoil, and therefore can lead to inaccurate results.

In other respect, three-dimensional Navier-Stokes fluid flow simulations have become affordable thanks to the increasing computation capabilities of the new generation of parallel computers. In this work, such a fluid flow solver is coupled with the structural model part of an aeroelastic code. It is thereby possible to perform more reliable numerical simulations of the fluid-structure interaction of a rotor with prescribed mode shapes of vibration. The mode shapes are determined from a modal analysis of the structure. Only the two first structural eigenmodes of the blades are considered in this study. Subsequently, the aerodynamic damping associated to these modes can be computed. The main objective of this new numerical model is to give a better understanding of the physical phenomena behind fluid-structure interaction and aeroelastic damping.

The paper is organized as follows. In the first section, both the fluid flow and structural numerical models are described, as well as their coupling. Thereafter, aeroelastic simulations and the methodology for computing the aerodynamic damping are exposed. Numerical experiments are conducted for a two-bladed wind turbine rotor. The results are analysed and conclusions are drawn concerning the differences between engineering dynamic stall models and full three-dimensional Navier-Stokes simulations.

2 NUMERICAL MODEL

This section is dedicated to the description of the the Navier-Stokes flow solver, and the original aeroelastic model. The coupling strategy is also emphasized.

2.1 Flow Solver

The fluid flow solver EllipSys3D has been used for this study. This in-house code was developed in co-operation between the Department of Mechanical Engineering at DTU (Technical University of Denmark) and the Department of Wind Energy at Risø National Laboratory. A detailed description of the numerical code can be found in the references.[5,6,13]

It is designed to solve the three-dimensional Navier-Stokes equations for an incompressible fluid. It uses a cell-centered grid arrangement for the pressure field and the cartesian velocity components. The equations are discretised by means of a finite volume formulation. The well-known velocity-pressure decoupling is circumvented by using the Rhie and Chow interpolation technique.[11] The SIMPLE algorithm is used for solving the momentum and pressure equations in a predictor-corrector fashion.[7] The Second order Upwind Differencing Scheme (SUDS) is applied to compute the convective fluxes,[15] whereas viscous terms are discretised with the classical second order central difference scheme. A subiteration technique is implemented in order to increase the critical time step.

The flow around a wind turbine is always somewhere turbulent. Therefore a turbulence model must be used in the fluid flow simulations. In our case, the $k-\omega$ SST turbulence model by Menter[4] in its original version was used to obtain the turbulent viscosity. The flow was assumed to be fully turbulent and no transition model was implemented.

As it will be described later, the deformation of the blades in the aeroelastic simulations implies a distortion of the computational grid which has to be considered in the numerical scheme. The convective fluxes are then given in Arbitrary Lagrangian-Eulerian (ALE) form[1] to take into account the local grid velocity.

The numerical code requires that the computational domain must be mapped onto a boundary-fitted structured grid. In order to facilitate the mapping and to take advantage of the new generation of parallel computers, a domain decomposition technique has been implemented in the numerical code. The meshes of the individual subdomains must be conformal, i.e. the grid lines must match at the interfaces between the subdomains. In a parallel computing platform, each processor is affected a certain number of subdomains. The communication between the several processors is performed by using the MPI-library.

2.2 Structural Model

The in-house made aeroelastic code HAWC is based on the finite element formulation[8,9] and is designed for simulating the dynamic response of horizontal axis wind turbines. The discretisation of the wind turbine structure is performed by use of prismatic, finite beam elements including two nodes each. Each node includes 6 degrees of freedom, corresponding to 3 translations and 3 rotations.

The kinematic analysis results in the accelerations of the material points of the structures, and subsequently the inertia loads. The inertia loads are consistently transformed to the nodes resulting in a matrix form of the equations of motion. In general, the resulting equations are non-linear due to product terms of degrees of freedom.

Structural damping is represented as proportional damping. The aerodynamic loading can be derived by use of an unsteady aerodynamic theory. For this purpose, two engineering semi-empirical dynamic stall models have been implemented in HAWC in order to perform aeroelastic simulations: the Beddoes-Leishman model,[3] and the Stig Øye model.[16]

The wind turbine is divided into three substructures comprising the tower, the shaft-nacelle and the rotor blades. In our case, only the rotor blades dynamics will be studied. In other words, the tower and the nacelle are considered as rigid. The aerodynamics around these substructures is neglected as well.

The aeroelastic code HAWC is also able to perform a modal analysis of the structure, giving access to the structural eigenmodes.

2.3 Coupling the Two Models

The core of this work is the computation of the aerodynamic damping for specific mode shapes of the structure. Therefore the coupling of the two models is relatively simple.

In a first step, the aeroelastic code HAWC is used to determine the vibration eigenmodes of the structure by performing a modal analysis of the considered wind turbine (see previous section). In our case, the modes are computed for a single non-rotating unloaded blade, i.e. all other components of the turbine are assumed totally rigid. Moreover, the structural damping of the blade is neglected.

In a second step, these structural modes are used to enforce a prescribed deformation of the blades. The blades oscillate according to a sinusoidal deflection of the modes with their own modal frequency. Moreover, the rotation of the rotor is superimposed on the deformation of the blades. The fluid flow solver can then be used to compute the flow field around the deforming rotor.

It must be noted that in the Navier-Stokes computations, the two blades are supposed to oscillate symetrically with respects to the center of rotation. In other words, if the deflection of one of the blades is positive in one direction relatively to its own coordinates system, the deflection of the other blade is negative in its own coordinates system, and vice-versa. Note that this has no influence in the case of the dynamic stall models, as the computed aerodynamic loads on the two blades has no influence on each others.

The deformation of the structure is taken into account in the flow solver by distorting the computational grid according to the blades deformation. In the vicinity of the blades, the grid is deformed as an elastic solid body, whereas in the farfield the grid is supposed to be fixed. In the intermediate regions between the blades, and between the individual blades and the farfield, arithmetic blending functions are used in order to ensure a resulting smooth distorted grid. This strategy has proven to give good results, even in the case of severe deformations of the blades. On the top of the previously described deformation, an overall rotation of the grid is superimposed to simulate the blade rotation.

3 COMPUTATION OF AERODYNAMIC DAMPING

The coupling of the two numerical codes has been described. It is now possible to perform aeroelastic simulations of a wind turbine rotor, and thereby predict the aerodynamic damping of this fluid/structure model.

3.1 Method

As mentioned before, the wind turbine model that is studied in the present work consists only of a two-bladed rotor. The influence of the tower and of the nacelle are neglected in all our computations. In the following, the mathematical derivation of the aerodynamic damping is described for one individual blade. Numerical experiments have actually proven that the flow dynamics is nearly identical for the two blades.

Aerodynamic damping can be deduced from the aerodynamic work exerted by the fluid on the blades. Given a station at radius r along a blade, the work performed by the fluid on an elementary blade section of size dr from time step $n-1$ to time step n can be computed as:

$$\Delta w(r)^n \, dr = \boldsymbol{F}^n \cdot \Delta \boldsymbol{X}^n \, dr \tag{1}$$

where $\boldsymbol{F}^n \, dr$ is the elementary aerodynamic force vector exerted on the blade section, computed by the fluid flow solver at the new time step n. The elementary displacement $\Delta \boldsymbol{X}^n$ of the structural nodes is given as:

$$\Delta \boldsymbol{X}^n = \boldsymbol{X}^n - \boldsymbol{X}^{n-1} \tag{2}$$

from the given displacement of the structural nodes $\boldsymbol{X}$ according to the modal shapes. The elementary work can be integrated in time by adding the contributions of n_p consecutive time steps, n_p being the number of time step required to cover one full period of the considered eigenmode. The aerodynamic work performed during this period on an elementary blade section dr thus reads:

$$w(r) \, dr = \sum_{n_p \text{ time steps}} \Delta w(r)^n \, dr \tag{3}$$

The logarithmic decrement of the local modal damping along the blade $\delta(r)$ is then given as:

$$\delta(r) \, dr = \frac{w(r) \, dr}{4\pi^2 M f^2 A^2} \tag{4}$$

where M is the modal mass of the blade, f is the frequency of the considered eigenmode, and A is the amplitude of the deformation (see for example Petersen *et al*[10] for a discussion on the computation of

	Mode 1 ($f = 7.3140\,Hz$)		Mode 2 ($f = 9.0755\,Hz$)	
Radius $[m]$	x-deflection $[m]$	y-deflection $[m]$	x-deflection $[m]$	y-deflection $[m]$
0.00	0.00	0.00	0.00	-0.00
1.00	$4.71.10^{-3}$	$2.24.10^{-2}$	$5.38.10^{-2}$	$-6.84.10^{-3}$
3.00	$6.13.10^{-2}$	$3.48.10^{-1}$	$4.33.10^{-1}$	$-6.19.10^{-2}$
4.00	$1.05.10^{-1}$	$6.44.10^{-1}$	$7.03.10^{-1}$	$-1.13.10^{-1}$
4.80	$1.42.10^{-1}$	$9.20.10^{-1}$	$9.33.10^{-1}$	$-1.65.10^{-1}$
5.03	$1.52.10^{-1}$	1.00	1.00	$-1.80.10^{-1}$

Table 1: Normalized Flapwise and Edgewise Eigenmodes of the Non-Rotating Blade

aerodynamic damping). Finally, the local modal damping can be integrated over the length of the blade to give the global modal damping:

$$\delta = \int_{\text{blade}} \delta(r)\, dr \tag{5}$$

for the considered eigenmode. Here and in the following, the term modal damping actually refers to the logarithmic decrement of the modal damping.

It must be noted that the computed unsteady fluid flow around the airfoil is not necessarily periodic, and even if it is, it is not necessarily a harmonic of the structural eigenmodes frequency. Moreover, it can take some time before the transient features damp out. Therefore the aeroelastic work is averaged over 4 periods of the structural deformation modes, and the averaging procedure starts approximately after 10 periods from the start of the simulation. It has been proven to be always enough to remove nearly all transient effects.

The procedure to compute the aerodynamic damping in the aeroelastic code HAWC is similar to the above described methodology. Namely, the structural eigenmodes are computed by a modal analysis, and thereafter aeroelastic simulations based on this mode shapes deformation are performed. The only difference is that the semi-empirical models are used to model the aerodynamic loads $\boldsymbol{F}$ instead of the Navier-Stokes fluid flow solver.

3.2 Numerical Example

The test case that has been chosen for this study corresponds to the Unsteady Aerodynamics Experiment Phase-VI rotor in NASA Ames Wind Tunnel by the National Renewable Energy Laboratory. The two-bladed $10.058\,m$ diameter Phase-VI rotor geometry is based on the S809 airfoil. All details about the blades can be found in Guiguere and Selig.[2] The wind speeds studied in the present work range from 5 to $25\,m/s$. The rotational speed of the rotor is $72\,rpm$. Note that for all the computations performed in this study, no yaw or tilt of the rotor is assumed.

The two first structural eigenmodes of the individual blades computed by HAWC are studied. The first mode corresponds to the first flapwise deformation mode, the second one to the first edgewise deformation mode of the blade. These modes and their respective eigenfrequencies are reported in Table 1. The x-axis represents the edgewise direction (in the rotor plane), positive from the trailing edge towards the leading edge of the blade. The y-axis is the wind flow direction in the coordinates system associated to the blade, for which z is the axis of the blade pointing towards the tip of the blade.

The amplitude of the modal deformation has been chosen such that the tip deflection is $0.1\,m$ in the main direction of the deformation (i.e. flapwise for mode 1, and edgewise for mode 2). This ensures that the deformations can be assumed small.

The discretisation chosen in the structural model for computing the structural eigenmodes includes 5 elements per blade (that is 10 nodes). However in the aeroelastic computations performed with HAWC in order to compute the aerodynamic damping, 12 elements per blade were used. The semi-empirical dynamic stall models are based on static lift and drag curves of the airfoil as a function of the angle of attack for the different airfoil sections where the discretisation nodes are located as an input. In our case, these curves originate from the experimental measurements performed by NREL.[12] They were however corrected according to our know-how on other airfoils in order to better match the experimental results.

The computational grid used to perform the Navier-Stokes simulations is composed of 20 blocks comprising 32 cells in each directions. As a consequence, the full computational grid involves 655,360 cells. The construction of this computational grid is described in Sørensen *et al.*[14] In order to reduce the computational costs, the grid used in the present study is actually a coarsened version of the original grid

where only every second grid point have been retained. Nevertheless, tests have shown that accuracy is satisfactory. The time step used for all computations is set to $\Delta t = 10^{-3}s$.

The density and the viscosity of the air were chosen respectively equal to $\rho = 1.224\,kg/m^3$ and $\mu = 1.784.10^{-5}\,kg/ms$, close to the conditions of the experiments.

3.3 Analysis of the Results

Firstly, the global aerodynamic damping for one blade as a function of wind speed is shown in Figure 1(a) for the first mode, and in Fig.1(b) for the second one. As it can be seen, the two dynamic stall models are in relatively good agreement with each other. As for the Navier-Stokes computations, the results differ noticeably. The first mode exhibits higher damping in the mid-range wind speed. The second mode exhibits lower damping in the mid-range and for high wind speed. It even predicts negative damping in the mid-range. However, the tendendies for all models are rather similar.

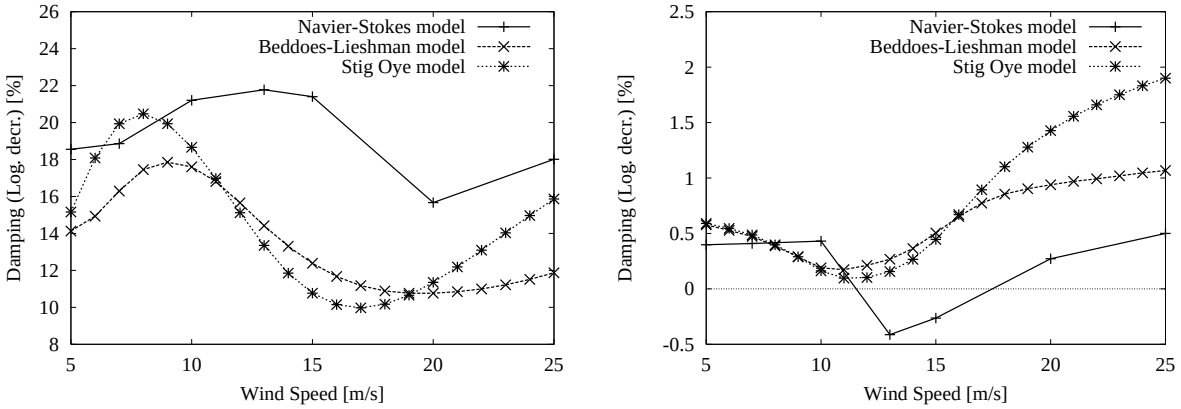

(a) Mode 1 (b) Mode 2

Figure 1: Aerodynamic Damping

In order to get a more detailed outlook of the results, the damping along one blade is considered next. Figs.2 and 3 show the damping along one blade for several wind speed for the Navier-Stokes computations and the semi-empirical dynamic stall models. It can first be noticed that the Navier-Stokes model has a particular behavior near the blade tip. Indeed, the damping drastically reduces when approaching the tip. As the deflection is maximum at the tip, it thus means that the aerodynamic forces vanish. There can be two obvious reasons. Firstly, as the chord of the blade shrinks at the tip, one can expect that the aerodynamic force will also vanish. Secondly, the three-dimensional flow field is known to be quite complex at the tip of an airfoil (due to tip vortex for example), therefore the aerodynamic forces are complex and difficult to predict in this region.

If one now looks at the general shape of the damping curves along the blade, the previous conclusions concerning the first mode are similar. Indeed, it can be seen on Fig.2 that damping computed from the Navier-Stokes model are significantly higher in the mid-range and for high wind-speeds. However, for all models curves have a similar shape. As for the second mode, the situation is a bit more complicated. The differences in the global damping can be found again in the local damping, but the shape of the different curves for the different models is not always similar. In particular, for the mid-range wind speed (Figs. 3(c-d-e)), it can be seen that the Navier-Stokes model predicts negative damping. Furthermore, this drop of damping can be observed in the middle of the blade. It is difficult to give a reason for this behavior without looking more carefully at the flow field behavior itself in this area, but it can be expected that highly detached flow, double stall or similar pattern may produce these results. Nevertheless, it can be seen that the dynamic stall model also predicts a reduced damping at some location along the blade, even if it is less pronounced. Interesting enough is the curves shape on Fig. 3(d) where all models predicts a second drop of the damping close to the tip, once again much less severe in the case of the dynamic stall models.

4 CONCLUSIONS AND PERSPECTIVES

The results obtained in this work are quite encouraging as for the reliability of our Navier-Stokes model. Indeed, the damping computed with this model for the chosen structural modes are in relative

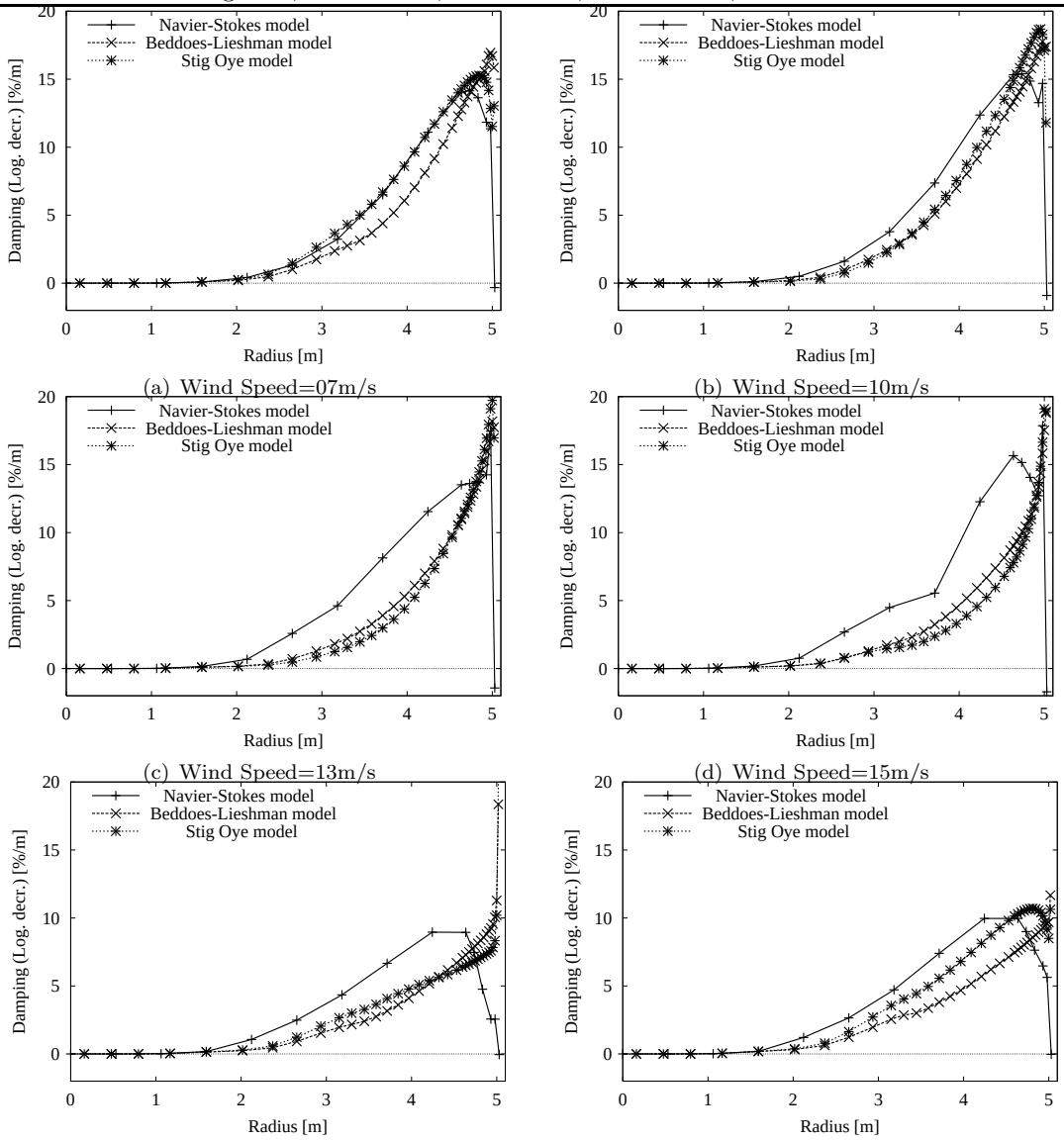

(a) Wind Speed=07m/s

(b) Wind Speed=10m/s

(c) Wind Speed=13m/s

(d) Wind Speed=15m/s

(e) Wind Speed=20m/s

(f) Wind Speed=25m/s

Figure 2: Aerodynamic damping along blade - Mode 1

good agreement, both qualitatively and quantitatively, with classical engineering models involving semi-empirical dynamic stall models. Nevertheless, some discrepancies were observed.

Our next objective is to understand why the results differ in some cases. Several ways of investigations are considered. Firstly, it is planed to compare the lift and drag loops at several stations along the blade were results do not fit well. Secondly, the semi-empirical dynamic stall models will get their static lift and drag curves from our Navier-Stokes model computations in order to get more consistent comparisons. Finally, negative damping has been predicted at some stations along the airfoil in disagreement with the dynamic stall models. The flow pattern predicted by the Navier-Stokes model in these regions will be closely investigated in order to understand if the dynamic stall models are unable to predict the actual physics of the flow.

ACKNOWLEDGEMENTS

This work was carried out under a contract with The Danish Energy Agency, ENS 1363/01-0001, Program for research in aeroelasticity 2001-2002. This research was also supported by the European Commission contract, KNOWBLADE, ENK6-CT-2001-00503. Computations were made possible by the use of the IBM RS/6000 SP at the Risø central computing facility.

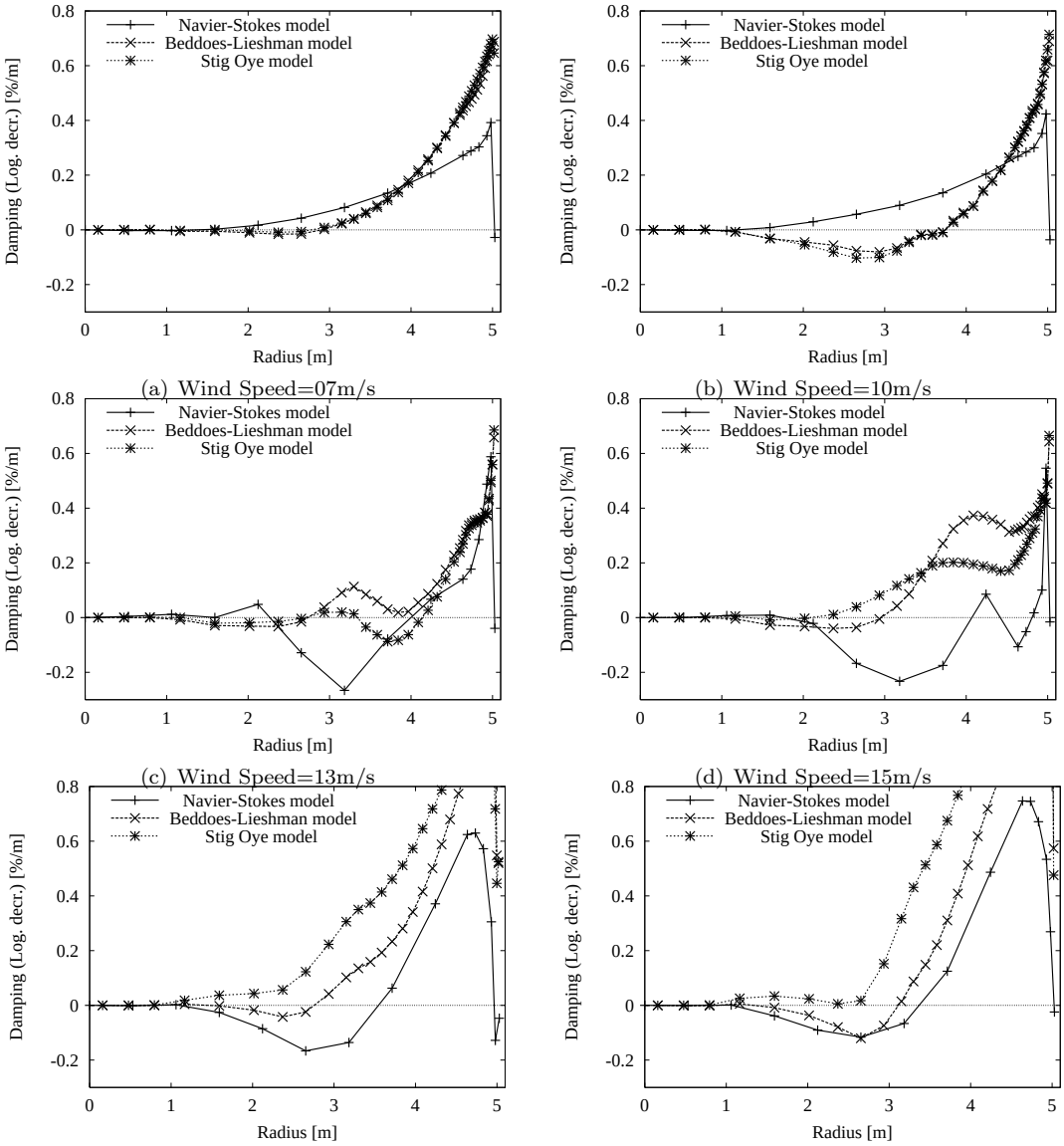

(a) Wind Speed=07m/s

(b) Wind Speed=10m/s

(c) Wind Speed=13m/s

(d) Wind Speed=15m/s

(e) Wind Speed=20m/s

(f) Wind Speed=25m/s

Figure 3: Aerodynamic damping along blade - Mode 2

References

[1] Donea J. (1982), "An Arbitrary Lagrangian-Eulerian Finite Element Method for Transient Fluid-Structure Interactions", Comput. Methods Appl. Mech. Eng., Vol.33, pp.689-723.

[2] Giguere P. and Selig M.S. (1999), "Design of a Tapered and Twisted Blade for the NREL Combined Experiment Rotor", Tech. Report, NREL/SR -500-26173, Nat. Renew. Energy Lab., Golden, CO.

[3] Leishman J.G. and Beddoes T.S. (1989), "A Semi-Empirical Model for Dynamic Stall", Journal of the American Helicopter Society, Vol.34, No.3, July 1989, pp.3-17.

[4] Menter F.R. (1993), "Zonal Two-Equations $k-\omega$ Turbulence Models for Aerodynamic Flows", AIAA Paper 93-2906.

[5] Michelsen J.A. (1992), "Basis3D - A Platform for Development of Multiblock PDE Solvers", Tech. Report, Technical University of Denmark, AFM 92-05.

[6] Michelsen J.A. (1994), "Block Structured Multigrid Solution of 2D and 3D Elliptic PDE's", Tech. Report, Technical University of Denmark, AFM 94-06.

[7] Patankar S.V. and Spalding D.B. (1972), "A Calculation Procedure for Heat, Mass and Momentum Transfer in Three-Dimensional Parabolic Flows", Int. J. Heat Mass Transfer, Vol.15, pp.1787-1806.

[8] Petersen J.T. (1990), "Kinematically Nonlinear Finite Element Model for a Horizontal Axis Wind Turbine", PhD Thesis, Risø National Laboratory, Roskilde, Denmark.

[9] Petersen J.T. (1996), "The Aeroelastic Code HAWC-Model and Comparisons", in *Proceedings of the* 28^{th} *IEA Experts Meeting: State of the Art of Aeroelastic Codes, Technical University of Denmark, Lyngby, 11-12 April.*

[10] Petersen J.T., Madsen H.A., Björck A, Enevoldsen P, Øye S., Ganander H. and Winkelaar D. (1998), "Prediction of Dynamic Loads and Induced Vibrations in Stall", Tech. Report, Risø National Laboratory, Roskilde, Denmark, Risø-R-1045(EN).

[11] Rhie C.M. and Chow W.L. (1983), "Numerical Study of the Turbulent Flow Past an Airfoil with Trailing Edge Separation", AIAA Journal, Vol.21, pp.1525-1532.

[12] Simms D., Schreck S., Hand M. and Fingersh L.J. (2001), "NREL Unsteady Aeordynamics Experiment in the NASA-Ames Wind tunnel: A Comparison of Predictions to Measurements", Tech. Report, NREL/TP -500-29494, Nat. Renew. Energy Lab., Golden, CO.

[13] Sørensen N.N. (1995), "General Purpose Flow Solver Applied to Flow over Hills", Tech. Report, Risø National Laboratory, Roskilde, Denmark, PhD Thesis, Risø-R-827(EN).

[14] Sørensen N.N., Michelsen J.A. and Schreck S. (2002), "Application of CFD to Wind Turbine Aerodynamics", in *Proceedings of the* 4^{th} *GRACM Congress on Computational Mechanics, Patras, 27-29 June.*

[15] Yeo R.W., Wood P.E. and Hrymak A.N. (1991), "A Numerical Study of Laminar 90-degree Bend Duct Flow with Different Discretization Schemes", J. Fluids Eng., Vol.113, pp.563-568.

[16] Øye S. (1990), "Dynamic Stall Simulated as Time Lag of Separation", in *Proceedings of the Fourth IEA Symposium on the Aerodynamics of Wind Turbines, Rome, 20-21 November.*